CRN STRASBOURG

CRN-PN/ 88-05

TEST OF COMPLEX EFFECTIVE INTERACTION BY FOLDING ANALYSIS OF ^{32}S ELASTIC SCATTERING ON s-d SHELL NUCLEI

B. Bilwès, R. Bilwès
Centre de Recherches Nucléaires et Université Louis Pasteur, Strasbourg, France

J. Díaz, J.L. Ferrero, J.C. Pacheco, J.A. Ruiz
Instituto de Física Corpuscular, Universidad de Valencia-CSIC, Burjasot, Valencia, Spain

CENTRE DE RECHERCHES NUCLEAIRES

STRASBOURG

IN2P3 CNRS

UNIVERSITE LOUIS PASTEUR

To be published in Nuclear Physics

TEST OF COMPLEX EFFECTIVE INTERACTION BY FOLDING ANALYSIS OF ^{32}S ELASTIC SCATTERING ON s-d SHELL NUCLEI *

B. BILWES, R. BILWES
Centre de Recherches Nucléaires and Université Louis Pasteur, Strasbourg, France.

J. DÍAZ, J. L. FERRERO, J. C. PACHECO and J. A. RUIZ
Instituto de Física Corpuscular, Universidad de Valencia-CSIC, Burjasot, Valencia, Spain.

Abstract: Experimental data of elastic scattering between nuclei of various structures on a large energy scale has been analyzed in the framework of the folding model by use of the complex effective interaction of Faessler et al (1981). A general good reproduction of the data is obtained if renormalization coefficients for the real and the imaginary parts of the optical potential are introduced. The application of the dispersion relation of Mahaux et al (1986) allows to reproduce the observed energy dependence of the real part of the potential.

NUCLEAR REACTIONS ^{32}S(^{32}S,^{32}S), E_{lab} = 70, 75, 90, 97.09, 120 and 160 MeV; ^{40}Ca(^{32}S, ^{32}S), E_{lab} = 90, 100, 110, 120 and 151.5 MeV; ^{34}S(^{32}S,^{32}S), E_{lab} = 77 , 90, 97.09 MeV; ^{28}Si(^{32}S,^{32}S), E_{lab} = 70, 77, 90, 97.09, 120 and 135 MeV; measured σ(E,θ), folding model analysis.

---

* Work partially supported by CAYCIT (Spain) under project PR84-0208 and by IN2P3-CNRS (France)

1. Introduction

The optical model has been a useful tool to describe heavy-ion and light-ion reactions. Usually the optical potential used to describe heavy-ion elastic scattering[1]) is parametrized by a complex Woods-Saxon form factor although many other phenomenological shapes are also employed to describe the real[2,3]) and the imaginary[2]) parts of the optical potential.

However, although the experimental data have been described adequately by means of a phenomenological parametrization the existence of ambiguities in the optical parameters makes it difficult to extract physical information. In order to try to remove these ambiguities much theorical effort has been done to determine the HI optical potential from the basic nucleon-nucleon interaction.

A simple and transparent relationship between the HI optical potential and the basic nucleon-nucleon interaction is obtained by using the double-folding model. In this way Satchler and Love[4]) have calculated the real part of the ion-ion potential by folding with the nuclear densities an effective nucleon-nucleon interaction derived from hermitian G-matrix elements based on the Reid soft-core potential[5]). As this effective interaction (M3Y) is real only the real part of the optical potential can be calculated by this model; the imaginary part of the optical potential must be treated phenomenologically.

In order to calculate the volume contribution to both the real and the imaginary parts of the optical potential a complex effective nucleon-nucleon interaction (CE) derived from non-hermitian G-matrix associated with a non-spherical Fermi sea has been recently proposed[6,7]). As the full calculations with the original form of the CE interaction are highly time consuming they could not be extended in practice to colliding systems heavier than $^{16}O + ^{16}O$ [7,8]). However a simplified form of the CE interaction has been derived[9]) to be used in the double-folding method of the optical potential computation which allows the extension of the analysis to heavier systems and to assymetric mass systems.

In a previous paper[11]) we compared the analysis of our experimental data[12,13,14]) obtained with the M3Y interaction to those obtained using the CE interaction. Two mass systems were considered at energies near the Coulomb barrier : $^{32}S + ^{32}S$ at 90 MeV and $^{32}S + ^{40}Ca$ at 100 MeV. We found that the CE interaction provides a reasonable description of the data, in comparison to those obtained when the M3Y interaction with a phenomenological imaginary part is used, if the imaginary part of the CE interaction is

renormalized.

In order to get a more systematic understanding of the mass and energy dependence on the potential we extended the analysis to more complete experimental data.

In this paper we analyse with the CE interaction our experimental data for four different systems: ^{32}S + ^{28}Si at 70, 77, 90, 97.09, 120 and 135 MeV; ^{32}S + ^{32}S at 70, 75, 90, 97.09, 120 and 160 MeV; ^{32}S + ^{34}S at 77, 90 and 97.09 MeV; ^{32}S + ^{40}Ca at 90, 100, 110, 120 and 151.5 MeV. Some of the experimental data are already published, others were measured to complete the energy range for this study: ^{32}S + ^{40}Ca at 90 MeV and 110 MeV; ^{32}S + ^{32}S at 75 MeV and ^{32}S + ^{28}Si at 70, 120 and 135 MeV.

2. Experimental procedure

The experiments have been performed at the MP accelerator of the CRN-Strasbourg. The targets were obtained either by the implantation technique[36]) in the case of ^{32}S and ^{34}S (2-3$\mu g/cm^2$) in carbon foils (20$\mu g/cm^2$) either by evaporation [37]) in the case of ^{40}Ca and enriched $^{28}SiO_2$ (20 $\mu g/cm^2$) on carbon foils (20 $\mu g/cm^2$).

The data have been taken using the kinematical identification method with two position-sensitive detectors mounted in coincidence, which has been described previously [12,15]).

The events were stored in steps of 1 degree in the CM system except at some backward angles where they were regrouped in 2 degree intervals [14]) because of the poor statistics. For each angular distribution two or three different geometrical arrangements of the detectors were sufficient to obtain the whole angular distributions. The error bars include both the statistical and the relative normalization errors between the different measurements. Absolute values of the elastic cross section were obtained by normalizing to the Rutherford scattering at the most forward angles.

3. Analysis

The double folding model describes the interaction between two colliding nuclei in the same way as the classical interaction between two static distributions of charge

$$V_F(r) = \int d\mathbf{r_1} d\mathbf{r_2} \rho_1(\mathbf{r_1}) \rho_2(\mathbf{r_2}) v_{CE}(r_{12})$$

where $r_{12} = |\mathbf{r} + \mathbf{r_2} - \mathbf{r_1}|$.

The densities $\rho(r_i)$ are deduced from experimental charge densities obtained mainly from electron scattering experiments (^{32}S,^{28}Si,^{40}Ca) or from proton scattering experiments (^{34}S) . As there exists evidence that for sd nuclei with N = Z it is reasonable to assume that the neutron and the proton distributions are identical[18]) the mass density was computed by scaling the charge density to the nuclear mass. The charge density was taken parametrized in the Fermi-parabolic form

$$\rho(r) = \rho_0 (1 + \omega \frac{r^2}{c^2}) \left(1 + \exp(\frac{r - c}{a})\right)^{-1}$$

In table 1 we include the values of these parameters for the different systems analysed [19,20,21,22]). The ρ_0 values were obtained by normalizing to the nuclear masses.

3.1. THE COMPLEX EFFECTIVE INTERACTION

The complex effective force [6,23]) was derived from the non-hermitian G-matrix obtained by solving the Bethe-Goldstone equation in the momentum space with a Reid soft-core potential corresponding to two nuclear matters with different densities streaming through each other. In contradistinction to the static matter case, two nucleons inside the Fermi sea can now suffer a real scattering which leads them to excited states above the Fermi surface. These 2p-2h excitations in the deformed sea distribution generate the imaginary part of the complex interaction. This complex force depends [23]) on the local matter density ρ , the energy at which the collision takes place and also on the spin and isospin. In practice this formulation of the CE interaction could not be extended to colliding systems heavier than ^{16}O + ^{16}O for the above mentioned reasons. This justifies the use of certain prescriptions that simplify the calculations. In this way the use of the Siemens prescription by Sartor and Faessler [9]) allows to define a local, spin and isospin-independent effective interaction which has been calculated for several Fermi sea configurations defined by different K_r, ρ and κ values. K_r is the relative momentum per nucleon which determines the distance between the spheres constituting the deformed Fermi sea, ρ is the total nuclear matter density which is defined at each given point by the sum of the densities of

the two colliding matters at this point (sudden density approximation) and κ is the ratio between the volume of the Fermi sea in the projectile not participating in the collision and the volume of the total Fermi sea.

Recently, different modifications have been introduced by Faessler et al.[10]) in order to describe in a consistent way the ground state properties of nuclei and the nuclei-nuclei potential. In particular a Weizsäcker term was introduced. This surface correction was shown to make the potential more attractive at large distances. Such a correction is not taken into account in the following calculations. We will discuss this point later. Moreover sudden and adiabatic approximations of the density were compared. The differences between both approximations are shown to be important only at small distances. However due to strong absorption scattering data are only sensitive to the tail of the potential. Taking sudden approximation in our analysis is therefore without consequence even if in our energy range the adiabatic approximation would be more correct.

A convenient parametrization of both the real and the imaginary parts of the complex effective interaction $v_{C\text{-}E}(r)$ is provided by the expression [9])

$$v_{C\text{-}E}(r) = \begin{cases} \frac{1}{x}(1 - e^{-2x})^2 e^{-3x} \sum_{m=0}^{6} A_m x^m & r < 1 \text{ fm} \\ \frac{1}{x}(1 - e^{-2x})^2 \sum_{m=1}^{7} Z_m e^{-mx} & r > 1 \text{ fm} \end{cases}$$

where $x = 0.7r$. The dependence of the interaction on the K_r, ρ and κ parameters is entirely contained in the A_m and Z_m coefficients which have been determined by a least square fit. These coefficients have been tabulated for various configurations corresponding to different values of the (K_r,ρ,κ) triplet[9]).

The volume contribution to the optical potential has been calculated by means of the RIHIOP code [24]) which computes both the real and the imaginary parts of the optical potential assuming the parametrized form of the interaction mentioned above. In this code it is considered that the real part of the potential is energy independent and that the imaginary part varies only linearly with energy. In order to adequate the numerical calculations to our energy range modifications in the published RIHIOP code have been introduced by Sartor [25]). Second order interpolation besides the third order used in the published code was introduced to calculate the A_m and Z_m coefficients for configurations (K_r,ρ,κ) not tabulated. This was done in order to estimate the errors on deduced values of N_n, N_w, and reaction cross sections (see below). Finally we added the possibility of using Fermi-parabolic densities.

When different interpolations between the A_m and Z_m coefficients tabulated in RIHIOP were used, the dispersion of the values of the fitted N_v and N_w factor was as large as 20 % (even 40 % in some cases). This means that the number of configurations for which the CE interaction is calculated is not sufficient.

3.2.OPTICAL MODEL CALCULATIONS

The theoretical angular distributions were computed with the ECIS code [20]. The integration step used was 0.05 fm and a sufficiently large number of partial waves was included in order to assure the convergence of the calculations.

As we have shown in the previous paper [11]) the bare CE interaction is not adequate to reproduce the experimental data. Introducing renormalization factors of the real part and more particularly of the imaginary part of the optical potential improved significantly the results. We adopt the same procedure in this paper.

In a first set of optical model calculations we have fixed to one the renormalization factor of the real part of the optical potential, N_v, and fitted the renormalization factor of the imaginary part of the optical potential, N_w, in order to reproduce the experimental data. In a second set of calculations we searched for the best values of both N_v and N_w factors starting from the results obtained in the first step that gave the best fit to the experimental data with $N_v = 1$. In all cases the search of the N_v and N_w values has been done in 0.01 steps. In this way the best renormalization coefficients at each energy were calculated.

In the following subsections we present the analysis done for each mass system.

3.2.1.THE ^{32}S + ^{40}Ca SYSTEM

In table 2 we give the calculated values of the N_v and N_w renormalization factors for the best fits as well as the corresponding reaction cross sections. In figure 1 we show the results obtained when only the imaginary part of the optical potential is renormalized (curve B) and when both the real and the imaginary parts of the optical potential are renormalized (curve A). As we can see with the renormalization of the imaginary part only

we cannot reproduce adequately the rainbow and the slope of the angular distributions (curve B). For this reason it was necessary to renormalize the real part (curve A) too. Better fits were then obtained in all cases . However, although the cross section at small angles is well predicted, the cross section calculated with the CE interaction decreases too quickly at large angles; this implies that to correct the imaginary part of the optical potential calculated with the CE interaction by introducing only a renormalization factor is not sufficient.

In figure 2 we compare the values of the reaction cross sections we calculated with phenomenological (Woods-Saxon) and microscopic [12]) (M3Y plus Woods-Saxon) potentials with those calculated with the CE interaction. The dispersion between the different values is close to 7%.

The dispersion relation [27,28,29]) predicts the real part values starting with the imaginary part values at the sensitivity radius region. The consistency between the real and the imaginary parts of the optical potential can be tested by comparing the predicted values to the "experimental" ones. The dispersion relation links the real and the imaginary potential through the expression

$$\Delta V_{E_S}(r;E) \quad (E \quad E_S)\frac{P}{\pi}\int_0^{\infty} \quad \frac{W(r;E')}{(E' \quad E_S)(E' \quad E)}dE'$$

where P is the principal value of the integral, E_S is an adequate reference energy and

$$\Delta V_{E_S}(r;E) \quad V(r;E) \quad V(r;E_S)$$

Assuming a linear schematic model for $W(E)$ we can represent it by n linear segments that join the "experimental" values. The integral can be calculated in that case and the result is [14])

$$\Delta V_{E_S}(r;E) = \frac{1}{\pi}\ln \frac{\prod_{i=0}^{n-1}\left|\frac{E_{i+1}-E}{E_i-E}\right|^{W_i(E)}\left|\frac{1}{E_n-E}\right|^{W_n}}{\prod_{i=0}^{n-1}\left|\frac{E_{i+1}-E_S}{E_i-E_S}\right|^{W_i(E_S)}\left|\frac{1}{E_n-E_S}\right|^{W_n}}$$

where

$$W_i(E) = \frac{W_{i+1} - W_i}{E_{i+1} - E_i}(E - E_i) + W_i$$

and (E_i, W_i) are the "experimental" points for the imaginary potential. The E_0 energy is assumed to be the value at which the imaginary potential vanishes i. e. $W(E_0) = 0$.

Figure 3 shows the results obtained with the dispersion relation taking 110 MeV as reference energy. As in the M3Y case [12]), an energy dependence of the renormalization factor is observed but the maximum value is less than 1 in the CE case. This means that the optical potential is too attractive. Some effects which seem to be more important than the introduction of a Weizsäcker surface correction [10]) have to be taken into account.

3.2.2. THE $^{32}S + ^{32}S$ SYSTEM

In table 2 we give the values obtained for the two renormalization factors, N_v and N_w, for the best fits and the corresponding reaction cross sections. In figure 1 we draw the results obtained when only the N_w renormalization factor is fitted (curve B) and when the two renormalization factors are fitted (curve A).

As it was the case with the M3Y interaction [14]) we found no sensitivity to the real part of the optical potential in the analysis of the 70 and 75 MeV data. In fact similar good fits of the experimental points can be obtained with very different values of the N_v factor.

For the higher energies the fits are approximately of the same quality as those obtained with the M3Y interaction [14]). In figure 2 we compare the values of the reaction cross sections obtained with different potentials[14,30]). A dispersion of less than 10% is obtained except at the lower incident energies where the sensitivity to the nuclear potential is very low. In figure 3 we represent the dispersion relation calculated as described previously for the $^{32}S + ^{40}Ca$ case by taking 160 Mev as reference energy. The maximum value of N_v is reached at a lower energy for the calculated curve than for the "experimental" points. The same observation could be made in the M3Y analysis[14]).

3.2.3. THE ^{32}S + ^{34}S SYSTEM

As shown in figure 4 this is not a "good" system to test the microscopic potentials because many oscillations are superimposed on the rainbow and the slope regions of the experimental data at 77 and 90 MeV. These oscillations have been reproduced in previous calculations by supposing a two nucleon transfer process between the two colliding nuclei[17]). Such a process can be well described by introducing an l-dependence in the real part of the optical potential. In order to avoid eventual errors on the normalization factors of the potential due to the superposition of potential scattering and elastic transfer we used the following parity dependent potential in our analysis:

$$V(r) = N_v V^R_{folding} + N_w W^I_{folding} + (-1)^l V_{pp} + V_c$$

Following the conclusions of ref. 38 a Yukawa form factor was chosen for the V_{pp} term. We used $V_{pp} = \alpha exp(-\beta r)/r$ with $\beta = (2\mu B)^{1/2}/\hbar$, B being the binding energy of the exchanged cluster, μ the reduced mass of the cluster-core system. In the present case $\beta = 1.3495$.

In a first step we discarded the parity dependent term and deduced the N_v and N_w factors by fitting only the forward part of the angular distributions in order to minimize the oscillation contributions; the 27.5 - 127.5 ° CM range was kept at 77 MeV, 31.5 - 98.5 ° CM range at 90 MeV and the 29.5 - 93.5 ° CM range at 97.09 MeV. Then the whole angular distributions were fitted by using the parity dependent potential. The N_v, N_w and α values and the total reaction cross sections are given in both cases in table 3.

In figure 4 curves B represent the best fits when the real and the imaginary parts are renormalized and curves A correspond to the best fits when a parity dependent potential is considered. The results obtained with the CE interaction are of the same quality as those obtained when the M3Y interaction and an l-dependent potential are used [30]) to describe the real part of the optical potential.

In figure 2 we compare the reaction cross sections calculated with different potentials having in every case a parity dependent real part[30]). A dispersion of the values of less than 10 % is observed. Fig. 5 shows the results obtained with the dispersion relation taking 97.09 MeV as reference energy. For energies below the Coulomb barrier the sensitivity to the nuclear part of the potential is weak. The high N_v value obtained at 77 MeV may be

related more to a Coulomb polarization potential than to a nuclear one.

3.2.4. THE ^{32}S + ^{28}Si SYSTEM

In figure 4 we can see that the experimental curves corresponding to the ^{32}S + ^{28}Si system present many oscillations. As in the preceeding case, they can be reproduced with the hypothesis of an elastic transfer[31]). For this reason the same procedure was adopted for the analyses. For this system β = 1.0788 with the previous definition. The curves are the results obtained by renormalizing both the real and the imaginary parts of the optical potential without (curve B) or with (curve A) a parity dependent part. The results are of similar quality as those obtained by using the M3Y interaction and an ℓ-dependent potential to describe the real part of the potential[31]).

In table 3 we give the reaction cross sections, the α values and the N_v and N_w renormalization factors corresponding to the best fits. The B sets were obtained by fitting only the experimental data in the region where the transfer oscillations are not of much importance; the 30.5 - 109.5° CM range at 77 MeV, the 34.5 - 107.9° CM range at 90 MeV and the 33.5 - 97.5° CM range at 97.09 MeV. At 70 MeV the complete distribution was analyzed. No attempt was done to fit the experimental data at 120 and 150 MeV with a parity dependent potential as no data at backward angles are available. In figure 2 we compare the reaction cross sections calculated with the CE interaction to those calculated with other potentials [16,31]). As in the preceeding cases the dispersion of the values is less than 10 % for energies above the Coulomb barrier. The "experimental" values of the real and imaginary potentials and the calculated curve for the real part with the dispersion relation are given in fig. 5. The reference energy is 97.09 MeV as the data at higher energies are of poorer quality.

4. Results and Conclusions

In order to test in various cases the folding potential calculated with the CE interaction we have analysed a great body of elastic scattering data of ^{32}S on s-d nuclei on a large incident energy range.

As oscillations at backward angles were observed in the case of ^{32}S + ^{34}S and ^{32}S + ^{28}Si, we introduced a parity dependent real part of the potential in their analysis. This

allows to take into account effectively the elastic transfer. In this way it was possible to compare the results obtained for all the systems which we have studied in the same conditions.

It has been found that it is necessary to renormalize the real and the imaginary parts of the optical potential calculated with the folding model when the CE interaction is used. In all cases we obtain a reasonable fit of the experimental data with only two parameters, almost of similar quality as those obtained when the renormalized M3Y interaction and a phenomelogical imaginary part were used [12,14,16,30]) i.e. where four parameters are needed. We have shown that the reaction cross sections calculated with the CE interaction are similar to those with the M3Y interaction or phenomenological potentials (Fig. 2).

The ideal situation of getting parameter free potentials is not yet reached but it is encouraging to have reduced to two the number of free parameters. In fact the results obtained for the N_r and the N_w renormalization factors must be discussed separately. We have found an energy dependence of N_r as we did with the M3Y interaction. The dispersion relation which links the real part of the potential at a given radius to the imaginary potential at the same distance was calculated at the sensitivity radius for each system. We found that it reproduces the general trend of the fitted renormalization factor. As an energy independent real potential is used in RIHIOP, this fact does not really constitute a test of the CE interaction but supports the hypothesis of the "threshold anomaly", that is the existence of a polarization potential at energies near the Coulomb barrier due to a rapid decrease of the absorption at these energies[27]). Nevertheless we can see on tables 2 and 3 that the values of N_r are not very different from unity at the higher energies where such a polarization potential is supposed not to exist. So although the real part of the optical potential calculated with the CE interaction does not include polarization effects, it is found to give a good description away from the threshold.

On the contrary the high values found for the N_w factor confirms that the CE interaction gives a too weak absorptive part[32]). Moreover for the $^{32}S + ^{40}Ca$ system we found that the renormalization of the imaginary potential by only a factor N_w is not sufficient. Not only the absolute value but also the slope of the imaginary potential has to be modified. This lack of absorption can be corrected by including a polarization potential obtained by taking into account the collective excitations which are important at low energies. This contribution can be calculated by using the projection method of Feshbach[32]) or by a coupled channel description[33,34]). The RIHIOP code allows in principle to calculate a surface potential by the first method. Unfortunately attempts to use this part of the code in our experimental conditions gave erroneous results.

Acknowledgments

We are greateful to Dr. Sartor for enlightening discussion and for adaptation to our needs in the RHHOP code and to L.Stuttgé for carefull reading of the manuscript.

References

(1) P. E. Hodgson, Nuclear Heavy-Ions Reactions (Oxford University Press 1977)

(2) U. N. Bragin and R. Donagelo, Nucl. Phys. **A433** (1985) 495

(3) G. R. Satchler, Direct Nuclear Reactions (Oxford University Press 1983)

(4) G. R. Satchler and W. G. Love, Phys. Reports **55** (1979) 183.

(5) G. Bertsch, J. Borysowicz, H. McManus and W. G. Love, Nucl. Phys. **A284** (1977) 399.

(6) T. Izumoto, S. Krewald and A. Faessler, Nucl. Phys. **A431** (1980) 319 ;Nucl. Phys. **A357** (1981) 471.

(7) R. Sartor, A. Faessler, S. B. Khadkikar, Nucl. Phys. **A359** (1981) 467.

(8) A. Faessler, L. Rikus and S. B. Khadkikar, Nucl. Phys. **A401** (1983) 157.

(9) R. Sartor and A. Faessler, Nucl. Phys. **A376** (1982) 263.

(10) N. Ohtsuka, R. Linden, F. B. Malik and A. Faessler, Nucl. Phys. **A465** (1987) 550.

(11) B. Bilwes, R. Bilwes, J. Diaz, J. L. Ferrero and J. C. Pacheco, J. of Phys. **G13** (1987) 975.

(12) A. Baeza, B. Bilwes, R. Bilwes, J. Diaz and J. L. Ferrero , Nucl. Phys. **A419** (1984) 412.

(13) B. Bilwes, R. Bilwes, J. Diaz, J. L. Ferrero, Nucl. Phys. A449 (1986) 519.

(14) B. Bilwes, R. Bilwes, F. Ballester, J. Diaz, J. L. Ferrero, C. Roldan, L. Stuttgé and F. Sanchez, Nucl. Phys. **A473** (1987) 353

(15) B. Bilwes, R. Bilwes, V. D'Amico, J. L. Ferrero, R. Potenza and G. Giardina, Nucl. Phys. **A408** (1983) 173.

(16) A. Baeza, J. Diaz, J. L. Ferrero, B. Bilwes, R. Bilwes and J. Raynal, Phys. Lett. **149B** (1984) 77 and Nucl. Phys. **A437** (1985) 93.

(17) M. C. Mermaz, B. Bilwes, R. Bilwes and J. L. Ferrero, Phys. Rev. **C27** (1983) 2408.

(18) W. S. Thompson and T. S. Eck, Phys. Lett. **67B** (1977) 151

(19) C. W. de Jager and H. de Vries, Nucl. Data Table **14** (1974) 479.

(20) G. C. Li, M. R. Yearian and I. Sick, Phys. Rev. **C9** (1974) 151.

(21) G. D. Alkhazov, S. L. Belostotsky, O. A. Domchenkov, Yu. V. Dotsenko, N. P. Kuropatkin, M. A. Schuvaev and A. A. Vorobyov, Phys. Lett. **57B** (1975) 47.

(22) R. F. Frosch, R. Hofstadter, J. S. McCarty, G. K. Nöldeke , K. J. Van Oostrum, M. R. Yearian, B. C. Clark, R. Herman and D. G. Ravenhall, Phys. Rev. **174** (1968) 1380.

(23) A. Faessler, T. Izumoto, S. Krewald and R. Sartor,Nucl. Phys. **A359** (1981) 509.

(24) A. Faessler, L. Rikus and R. Sartor, Comp. Phys. Comm. **28** (1983) 275.

(25) R. Sartor, Private communication.

(26) J. Raynal, Phys. Rev. **C23** (1981) 2571.

(27) C. Mahaux, H. Ngô and G. R. Satchler, Nucl. Phys. **A449** (1986) 354.

(28) C. Mahaux, H. Ngô and G. R. Satchler, Nucl. Phys. **A456** (1986) 134.

(29) M. A. Nagarajan, C. Mahaux and G. R. Satchler, Phys. Rev. **C54** (1985) 1136.

(30) C. Roldan, Tesis Doctoral, Univ. de Valencia 1987.

(31) B. Bilwes, R. Bilwes, J. Díaz, J. L. Ferrero, D. Počanić and L. Stuttgé, Nucl. Phys. **A463** (1987) 731.

(32) S. B. Khadkikar, L. Rikus, A. Faessler and R. Sartor, Nucl. Phys. **A369** (1981) 495.

(33) A. Faessler, W.H. Dickhoff and M. Trefz, Nucl. Phys. **A428** (1984) 271c.

(34) M. Trefz, A. Faessler and W. H. Dickhoff, Nucl. Phys. **A443** (1985) 499.

(35) L. Stuttgé,Thesis,Univ. of Strasbourg (1985).

(36) *in collaboration with* J. Chaumont, R. Meunier, Laboratoire Bernas.Orsay.

(37) M. A. Saettel, C. R. N. *Strasbourg.*

(38) P. J. A. Buttle and L. J. B. Goldfarb, Nucl. Phys. **A115** (1968) 461; W. von Oertzen, Nucl. Phys. **A148** (1970) 529; D. Baye, Nucl. Phys. **A460** (1986) 581.

Table 1: Values of the ρ_o, w, c and a parameters for the ^{28}Si, ^{32}S, ^{34}S and ^{40}Ca nuclei

NUCLEUS	ρ_o(nucleon/fm^3)	w	c (fm)	a(fm)	Ref.
^{28}Si	0.1775	-0.149	3.239	0.574	19
^{32}S	0.1825	-0.213	3.441	0.624	20
^{34}S	0.1860	-0.213	3.470	0.647	21
^{40}Ca	0.1701	-0.1017	3.6758	0.585	22

Table 2 : Best fit parameters for the CE interaction for the $^{32}S + ^{40}Ca$ and the $^{32}S + ^{32}S$ systems

$^{32}S + ^{40}Ca$						$^{32}S + ^{32}S$					
E_{lab}	CURVE	N_V	N_W	χ^2/N	σ_R	E_{lab}	CURVE	N_V	N_W	χ^2/N	σ_R
90	A	0.80 †	27.26	7.60	509	70	A	5.41 †	7263.12	2.25	290
	B	1.	14.25	14.02	480		B	1.	6077.93	2.27	266
100	A	0.79 †	21.2	45.60	773	75	A	1.95	619.58	16.84	406
	B	1.	17.1	67.20	778		B	1†	595.75	17.21	388
110	A	0.64 †	32.99	12.54	1057	90	A	0.88	28.29	3.66	666
	B	1.	3.70	63.44	904		B	1†	21.88	4.33	664
120	A	0.54 †	29.91	14.13	1230	97.09	A	0.93	25.60	3.09	844
	B	1.	89.19	52.97	1449		B	1†	23.96	3.40	848
151.5	A	0.57 †	22.58	6.88	1656	120	A	0.96	30.09	3.80	1300
	B	1.	57.30	27.15	1865		B	1†	31.17	3.87	1308
						160	A	0.64	9.98	5.09	1552
							B	1†	11.13	47.75	1630

† parameters not fitted

Table 3 : The same as table 2 for the $^{32}S + ^{34}S$ and $^{32}S + ^{28}Si$ systems

$^{32}S + ^{34}S$							$^{32}S + ^{28}Si$						
E_{lab}	CURVE	N_V	N_W	a	χ^2/N	σ_R	E_{lab}	CURVE	N_V	N_W	a	χ^2/N	σ_R
77	B	1.51	62.70	0†	9.04	458	70	B	1.09	43.98	0†	2.24	141
	A	1.68	6.83	-275.10^4	12.81	394		A	1.09	43.26	-40.10^4	2.20	141
90	B	1.19	27.44	0†	7.77	792	77	B	1.01	115.07	0†	4.39	452
	A	1.19	25.24	-121.10^4	7.80	787		A	1.05	55	-25.10^4	17.50	401
97.09	B	1.04	27.99	0†	5.71	954	90	B	0.87	58.85	0†	5.58	769
	A	1.04	21.23	-32.10^4	7.81	930		A	0.88	57.91	-18.10^4	5.75	768
							97.09	B	0.9	46.36	0†	2.35	921
								A	0.93	47.05	-3.10^4	2.28	930
							120	B	0.94	26.31		0.56	1259
							135	B	1.06	28.98		1.82	1465

† parameters not fitted

Figure captions

Fig. 1 :*Left:* Comparison between the experimental data for $^{32}S + ^{40}Ca$ at 90,100,110,120 and 151.5 Mev laboratory energies and theoretical predictions using the folding model with a complex effective (CE) interaction. Curves obtained with renormalized real and imaginary parts (full line) and only the imaginary part (broken line) of the optical potential are given.*Right:* The same for the $^{32}S+^{32}S$ system at 70,75,90,97.09,120 and 160 MeV laboratory energies.

Fig. 2 : Comparison between the reaction cross sections calculated with only a Woods-Saxon form factor (○); with the M3Y interaction plus a Woods-Saxon form factor (△) and with the renormalized CE interaction (□) for $^{32}S+^{40}Ca$,$^{32}S+^{32}S$, $^{32}S+^{34}S$ and $^{32}S+^{28}Si$ at various incident energies. The opened or closed symbols and the lines are only for guiding eyes.

Fig. 3 :*Left:* The values of the real and the imaginary parts of the optical potential at 10 fm for the $^{32}S + ^{40}Ca$ system and predicted real part by the dispersion relation.The curve for the real part has been calculated with a 2 segment imaginary part .We considered that the imaginary potential vanishes at 70 MeV. The 110 MeV was taken as the reference energy. The values of the renormalization factors are given on the right scale. *Right:*. The same for the $^{32}S+^{32}S$ system at 9.4 fm. The curve for the real part has been calculated with the values of the imaginary part linked by the drawn curve. We considered that the imaginary potential vanishes at 60 MeV. The 160 MeV was taken as the reference energy.

Fig. 4 :*Left:* Comparison between the experimental data for $^{32}S+^{34}S$ and theoretical predictions using the folding model with the CE interaction. Curves obtained with renormalized real and imaginary parts without parity dependence (broken line) and with parity dependence (full line) of the optical potential are given. *Right:* The same for $^{32}S+^{28}Si$.

Fig. 5 :*Left:* The same as Fig. 3 for the $^{32}S + ^{34}S$ system at 9.6 fm. We considered that the imaginary potential vanishes at 70 MeV. The reference energy taken was 97.09 MeV. *Right:* The same as Fig. 3 for the $^{32}S + ^{28}Si$ system at 9.2 fm. The reference energy was 97.09 MeV The imaginary potential was considered to vanish at 52 MeV.

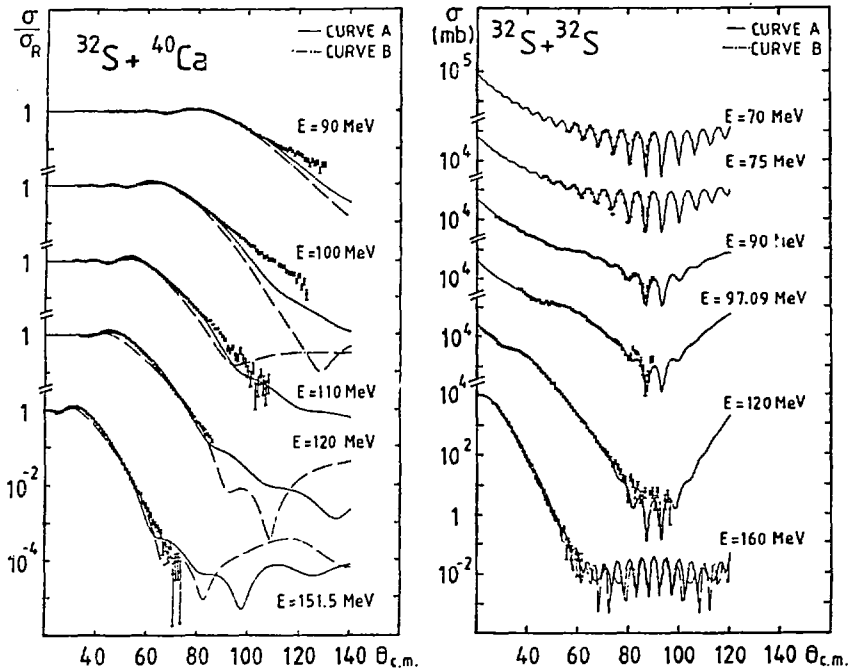

Figure 1

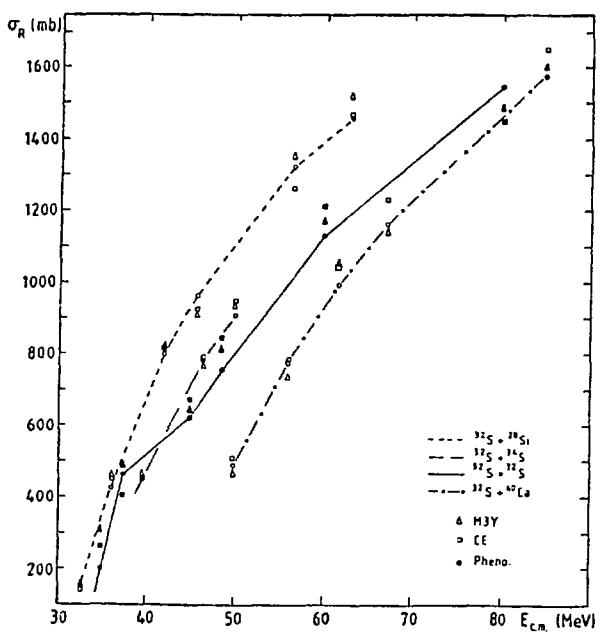

Figure 2

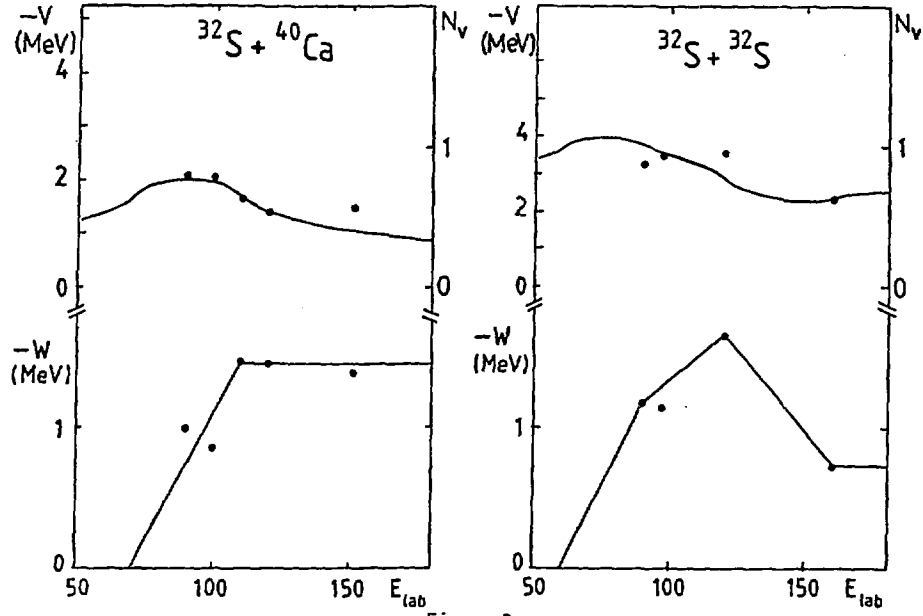

Figure 3

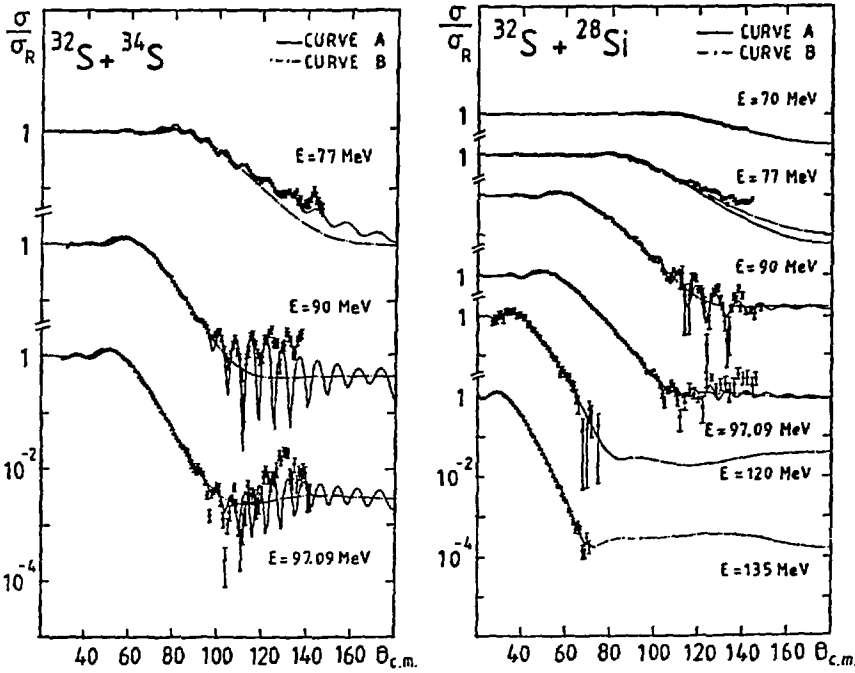

Figure 4

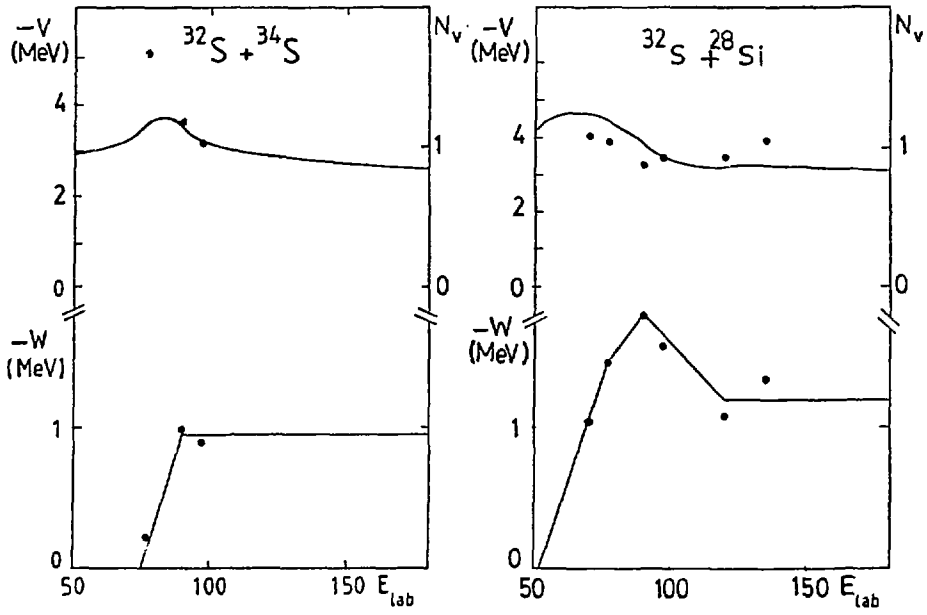
−V (MeV)
$^{32}S + ^{34}S$
N_v
4
2
0
1
0
−W (MeV)
1
0
50
100
150 E_{lab}
−V (MeV)
$^{32}S + ^{28}Si$
N_v
4
2
0
1
0
−W (MeV)
1
0
50
100
150 E_{lab}

Figure 5

Imprimé
au Centre de
Recherches Nucléaires
Strasbourg
1988